European Radiology (2019) 29:759–769
https://doi.org/10.1007/s00330-018-5655-0

NEURO

Detection of suspected brain infarctions on CT can be significantly improved with temporal subtraction images

Thai Akasaka[1] · Masahiro Yakami[1,2] · Mizuho Nishio[1,2] · Koji Onoue[1] · Gakuto Aoyama[3] · Keita Nakagomi[3] · Yoshio Iizuka[3] · Takeshi Kubo[1] · Yutaka Emoto[4] · Kiyohide Satoh[3] · Hiroyuki Yamamoto[5] · Kaori Togashi[1]

Received: 3 April 2018 / Revised: 26 June 2018 / Accepted: 4 July 2018 / Published online: 30 July 2018

Abstract

Objective To assess whether temporal subtraction (TS) images of brain CT improve the detection of suspected brain infarctions.

Methods Study protocols were approved by our institutional review board, and informed consent was waived because of the retrospective nature of this study. Forty-two sets of brain CT images of 41 patients, each consisting of a pair of brain CT images scanned at two time points (previous and current) between January 2011 and November 2016, were collected for an observer performance study. The 42 sets consisted of 23 cases with a total of 77 newly developed brain infarcts or hyperdense artery signs confirmed by two radiologists who referred to additional clinical information and 19 negative control cases. To create TS images, the previous images were registered to the current images by partly using a non-rigid registration algorithm and then subtracted. Fourteen radiologists independently interpreted the images to identify the lesions with and without TS images with an interval of over 4 weeks. A figure of merit (FOM) was calculated along with the jackknife alternative free-response receiver-operating characteristic analysis. Sensitivity, number of false positives per case (FPC) and reading time were analyzed by the Wilcoxon signed-rank test.

Results The mean FOM increased from 0.528 to 0.737 with TS images ($p < 0.0001$). The mean sensitivity and FPC improved from 26.5% and 0.243 to 56.0% and 0.153 ($p < 0.0001$ and $p = 0.239$), respectively. The mean reading time was 173 s without TS and 170 s with TS ($p = 0.925$).

Conclusion The detectability of suspected brain infarctions was significantly improved with TS CT images.

Key Points

- *Although it is established that MRI is superior to CT in the detection of strokes, the first choice of modality for suspected stroke patients is often CT.*
- *An observer performance study with 14 radiologists was performed to evaluate whether temporal subtraction images derived from a non-rigid transformation algorithm can significantly improve the detectability of newly developed brain infarcts on CT.*
- *Temporal subtraction images were shown to significantly improve the detectability of newly developed brain infarcts on CT.*

Keywords Multidetector computed tomography · Stroke · Brain infarction · Computer assisted diagnosis · Subtraction technique

Electronic supplementary material The online version of this article (https://doi.org/10.1007/s00330-018-5655-0) contains supplementary material, which is available to authorized users.

✉ Thai Akasaka
thai.akasaka@gmail.com; takasaka@kuhp.kyoto-u.ac.jp

[1] Diagnostic Imaging and Nuclear Medicine, Kyoto University Graduate School of Medicine, 54 Kawahara-cho, Shogoin, Sakyo-ku, Kyoto, Kyoto 606-8507, Japan

[2] Preemptive Medicine and Lifestyle-Related Disease Research Center, Kyoto University Hospital, 53 Kawahara-cho, Shogoin, Sakyo-ku, Kyoto, Kyoto 606-8507, Japan

[3] Medical Imaging System Development Center, R&D Headquarters, Canon Inc., 30-2, Shimomaruko 3-chome, Ohta-ku, Tokyo 146-8501, Japan

[4] Kyoto College of Medical Science, 1-3 Imakita, Koyamahigashi-cho, Sonobe-cho, Nantan, Kyoto 622-0041, Japan

[5] Business Development Promotion Center, Corporate Planning Headquarters, Canon Inc., 30-2, Shimomaruko 3-chome, Ohta-ku, Tokyo 146-8501, Japan

Abbreviations

ADC	Apparent diffusion coefficient
AFROC	Alternative free-response receiver operating characteristic
CAD	Computer-aided detection
CCL	Cerebral cortex lesion
CNR	Contrast-to-noise ratio
DWI	Diffusion-weighted imaging
DWML	Deep white matter lesion
EHL	Early hyperacute lesion
FLAIR	Fluid attenuation inversion recovery
FOM	Figure of merit
FPC	False positives per case
GPU	Graphics processing unit
HAS	Hyperdense artery sign
JAFROC	Jackknife alternative free-response receiver operating characteristic
LDDMM	Large deformation diffeomorphic metric mapping
SNR	Signal-to-noise ratio
TS	Temporal subtraction

Introduction

The detection of fresh brain infarctions on CT is often a challenging task for several reasons. First, for the infarcted brain tissue to be conspicuous on CT, at least 6 h from onset must elapse. Prior to this, the infarcted lesions may be depicted as subtly attenuated areas known as early CT signs, but considerable expertise is required for their detection [1–4]. Second, previous infarcts and chronic ischemic changes, which are likely present in patients with a high risk of ischemic events, often obscure fresh infarcts, especially in the deep white matter. Third, CT is prone to beam-hardening artifacts, which often hinder the detection of infarcts, particularly in the brain stem [5, 6]. MRI suffers less from these disadvantages because DWI, and especially ADC maps, can elucidate fresh infarcts as rapidly as within an hour after onset in some cases [7]. Naturally, it is well established that MRI outperforms CT in the detection of strokes [8, 9]. Nevertheless, CT remains the first choice in many medical institutions due to its shorter acquisition time, better accessibility, fewer contraindications and lower cost [10].

The TS technique is one of the CAD techniques in which images are obtained by subtraction of two different sets of CT images to enhance the interval changes between them (hereafter, the two sets of CT are referred to as previous and current CTs). The two images must be registered before subtraction can be performed, and this can roughly be done in three ways—rigid, affine or non-rigid registration [11]. With rigid or affine transformation, subtle changes such as progression of brain atrophy or dilatation of the ventricles cause misregistrations, whereas non-rigid registration can cope with these subtle changes and generate higher quality subtraction images (Fig. 1).

TS has been shown to improve the detection of lung nodules on plain radiographs and thoracic CT, and TS with non-rigid registration similar to the method used in our study has been shown to improve detection of bone metastases on CT [12–15]. However, to the best of our knowledge, there is no report that has applied a TS technique to brain CT for the detection of newly developed brain infarcts. In this study we developed a TS technique for brain CT by use of a non-rigid image registration algorithm called LDDMM [16] and assessed whether TS images of brain CT can improve the detection of newly developed brain infarcts.

Materials and methods

Subject population

Our clinical database was searched for radiology reports written between January 2011 and November 2016 with "infarct" as the keyword and "MR" as the modality. Next, for each candidate sequentially, pairs of brain CT images were searched that

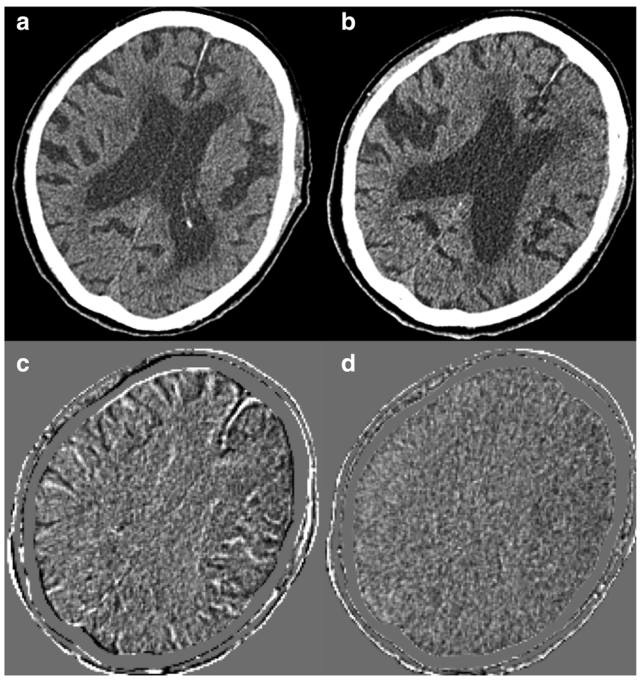

Fig. 1 Comparison of two temporal image subtraction techniques: rigid and non-rigid transformations. The (**a**) previous CT, (**b**) current CT, (**c**) TS CT using rigid registration only and (**d**) TS CT using rigid registration refined with non-rigid registration (in this case, LDDMM) are shown. Rigid transformation and subtraction causes minor misregistrations of the brain sulci, whereas LDDMM and subtraction can cope with these subtle changes and generate better subtraction images

matched the following criteria: (1) scanned at two distinct time points, (2) stored as thin-slice images (≤ 1 mm), (3) the presence of at least one low density area, regardless of size, in the brain parenchyma depicted only on the current CT, suggestive of a newly developed infarct between the two time points and (4) the absence of any focal lesions other than infarcts, such as tumor or hemorrhage. The exclusion criterion was TS image generation failure. The selected image pairs were retrospectively reviewed, and their lesions were confirmed by consensus of two radiologists. The confirmation of an infarction was achieved by identifying high signal intensities in the suspected infarcted area on DWI (B = 1000) images and lower apparent diffusion coefficient values relative to the surrounding brain parenchyma when DWI images scanned within 5 days before or after the current CT were available or by identifying isolated high signal intensities in the suspected infarcted area on FLAIR images scanned after the current CTs were available. Additionally, all available clinical information including charts and future images was referred.

As control cases, our database was sequentially searched for pairs of brain CT images scanned between April 2013 and October 2016 that matched the first, second and fourth criteria for infarction-positive cases, but with no apparent newly developed infarcts.

Subset analysis

To investigate whether our TS technique can enhance the detection of not only old infarcts that developed between the current and previous CTs but fresh infarcts as well, a subset of the whole data set was created whose positive cases consisted only of infarcts confirmed by DWI. The control group was kept the same. In addition, the following lesions were searched from the whole data set, and their subset analyses were performed: HAS, defined as a high-density area on the cerebral artery indicative of a thrombus; EHL, defined as an infarct depicted as a vaguely attenuated area on the current CT, which was scanned less than 6 h after onset, whose location matched the high signal intensity on DWI images and suspected of causing the symptom; CCL, defined as an infarct that was mainly located on the cerebral cortex; DWML, defined as an infarct that was located in the deep white matter. All lesions were determined by consensus of two radiologists.

Temporal subtraction technique

TS images were generated in brief by the following steps: (1) registration of the previous CTs to the current CTs by rigid transformation followed by LDDMM and (2) subtraction of the transformed previous CTs from current CTs. The details of the image processing are described in the online supplement material.

Image interpretation session

Fourteen readers consisting of 11 radiologists and 3 radiology residents with 3–25 years of clinical experience independently interpreted two groups of thin-slice brain CT images: (A) 42 sets of current and previous CTs and (B) 42 sets of current, previous and TS CTs. An in-house image viewer running on a Windows PC (Windows 10, Intel Core i7, 16 GB RAM) was used for the interpretation session. To reduce memory bias, seven randomly assigned and seven remaining readers were scheduled to interpret image groups A and B in their first session and then B and A in the second session, respectively, with an interval of more than 4 weeks between the two sessions. The order of the image sets was randomized for each reader. To control practice effects, readers were trained to the image viewer using six training cases prior to an actual observer study. The readers were blinded to all clinical data. The readers were asked to mark suspicious newly developed brain infarcts and intracranial thrombi with a likelihood level of diagnosis (1 to 100%). No limits were set for the size of the lesion to mark or for the time allowed for interpretation of the images. If a single lesion was considered marked several times, the mark with the highest likelihood level was treated as the response. After interpretation of each case, the readers were asked to rate the confidence level of their interpretation (survey 1: 1, very low; 2, low; 3, moderate; 4, high; 5, very high) and the usefulness of TS images (survey 2: 1, useless; 2, not very useful; 3, somewhat useful; 4, very useful; 5, extremely useful) for each case. Reading time for each case was recorded.

Statistical analysis

The lesion-based sensitivity, case-based sensitivity and specificity, number of FPC, reading time and confidence level were compared between the two sessions using the Wilcoxon signed-rank test. For lesion-based analysis, a lesion with 51% or higher likelihood of being an infarct was considered positive. For case-based analysis, cases with at least one positive lesion were considered positive. To evaluate observer performance, an FOM, equivalent to the area under the AFROC curve, was calculated along with the JAFROC analysis. Simply put, the AFROC curve is a lesion-based version of the ROC, which is a case-based analysis [17, 18]. The analysis was conducted using the freely available JAFROC software (JAFROC, version 4; http://www.devchakraborty.com) with a random-readers and random-cases model [18]. Changes in the sensitivity for HAS, EHL, CCL and DWML

Table 1 List of all infarction-positive cases and lesions used for the observer performance study

Patient	Age	Sex	Symptoms	Elapsed time (h)	Number of lesions	Size (mm)	Location	Confirmed by					
								DWI	FLAIR	HAS	EHL	CCL	DWML
1	90	F	Weakness of right hand	100-110	5	12.7	Lt. frontal cortex	○	○				
						22.9	Rt. cerebellar hemisphere	x	○				
						14.4	Rt. cerebellar hemisphere	x	○				
						5.6	Rt. cerebellar hemisphere	x	○				
						17.9	Lt. occipital cortex	x	○			✓	
2	92	F	Right hemiparalysis	47-48	2	12.1	Lt. frontal cortex	○	x			✓	
						22.8	Lt. cerebellar hemisphere	x	○				
3	72	M	Dysbasia, left hemiparesis	6	2	-	Rt. anterior cerebral artery	x	x	✓			
						35.0	Rt. frontal cortex	○	-		✓	✓	
3	72	M	Dysbasia, left hemiparesis	120	3	7.6	Rt. frontal cortex	○	○			✓	
						35.0	Rt. frontal cortex	○	-			✓	
						22.0	Rt. frontal cortex	○	○			✓	
4	78	F	Impaired consciousness	Unknown	7	6.8	Rt. frontal cortex	○	○			✓	
						13.2	Rt. frontal white matter	○	○				✓
						12.7	Lt. frontal white matter	○	○				✓
						33.4	Rt. parietal cortex	○	○			✓	
						12.8	Rt. parietal cortex	○	○			✓	
						6.7	Rt. cerebellar hemisphere	○	○				
						7.2	Lt. cerebellar hemisphere	○	○				
5	60	M	Aphasia, right hemiparalysis	<4	2	-	Lt. middle cerebral artery	x	x	✓			
						117.0	Lt. cerebral hemisphere	○	x		✓		
6	67	M	Dysarthria, left upper limb paralysis	0.5	8	5.5	Rt. parietal cortex	○	○			✓	
						7.6	Lt. occipital white matter	○	○				
						6.8	Lt. occipital cortex	○	○			✓	
						12.5	Rt. cerebellar hemisphere	○	○				
						7.1	Rt. cerebellar hemisphere	○	○				
						6.1	Rt. cerebellar hemisphere	○	○				
						3.9	Rt. frontal white matter	○	○				
						4.6	Rt. frontal white matter	○	○				
7	79	F	Aphasia	144-150	4	7.4	Lt. frontal white matter	○	○				
						5.7	Lt. basal ganglia	○	○				
						12.3	Rt. corona radiata	○	○				✓
						4.2	Rt. corona radiata	○	○				✓
8	82	M	Weakness of right upper limb	72-78	3	6.4	Lt. parietal cortex	○	x			✓	
						2.9	Lt. corona radiata	○	x				✓
						9.9	Lt. frontal white matter	○	○				
9	91	M	Sudden collapse, dysarthria	42-44	5	8.0	Lt. parietal cortex	○	○			✓	
						19.3	Lt. thalamus	○	○				
						20.5	Lt. hippocampal tail	○	○				
						17.0	Lt. occipital cortex	○	○			✓	
						10.8	Lt. lateral white matter	○	○				
10	89	F	Left hemiparesis	110-120	1	5.7	Rt. frontal cortex	○	○			✓	✓
11	86	F	Weakness of left limbs	20-24	3	7.9	Rt. insular white matter	○	x				

Table 1 (continued)

Patient	Age	Sex	Symptoms	Elapsed time (h)	Number of lesions	Size (mm)	Location	Confirmed by					
								DWI	FLAIR	HAS	EHL	CCL	DWML
						7.6	Rt. frontal white matter	○	x				✓
						7.0	Rt. corona radiata	x	○				✓
12	77	F	Numbness of lips	28-32	3	14.4	Rt. thalamus	○	○				
						18.4	Lt. hippocampus	○	○				
						16.4	Rt. occipital cortex	○	○			✓	
13	11	F	Postoperative state of moyamoya disease	15-20	1	43.3	Lt. parietal cortex	○	○			✓	
14	77	M	Loss of consciousness during medical treatment, aphasia, right hemiparalysis	1.5	2	30.6	Rt. frontal white matter	○	○				
						20.7	Lt. frontal white matter	○	○				
15	72	M	Collapsed, unconsciousness	9-10	1	28.6	Lt. insular cortex	○	○			✓	
16	92	M	Impaired consciousness, worsening of right upper limb paresis	2	2	48.1	Lt. cerebral hemisphere	○	x		✓		
						-	Lt. middle cerebral artery	x	x	✓			
17	78	F	Sudden weakness of right upper limb	5.5	1	19.9	Lt. lateral cortex	○	x		✓	✓	
18	83	F	Unknown	Unknown	10	14.0	Splenium of the corpus callosum (rt.)	○	○				
						8.1	Splenium of the corpus callosum (lt.)	x	x				
						3.8	Lt. corona radiata	x	○				✓
						4.1	Rt. thalamus	x	x				
						6.2	Lt. thalamus	x	○				
						9.6	Lt. hippocampus	x	x				
						16.2	Pons (rt.)	x	x				
						18.0	Rt. cerebellar hemisphere	x	x				
						37.9	Lt. cerebellar hemisphere	x	x				
						6.1	Pons (lt.)	x	x				
19	88	F	No response to call	6-14	2	16.7	Rt. parietal cortex	○	○			✓	
						6.1	Lt. cerebellar hemisphere	○	x				
20	81	F	General fatigue, loss of strength	6-12	1	4.4	Rt. basal ganglia	x	○				
21	80	F	Dysarthria, right hand paresis	6-8	8	5.6	Rt. corona radiata	x	x				✓
						5.0	Rt. basal ganglia	x	○				
						4.4	Lt. basal ganglia	x	○				
						4.3	Rt. basal ganglia	x	x				
						5.3	Rt. occipital cortex	○	○			✓	
						22.9	Rt. cerebellar hemisphere	x	○				
						12.7	Pons (lt.)	○	○				
						5.3	Rt. cerebellar hemisphere	x	○				
22	85	M	Left hemiparalysis	4.5	1	34.2	Rt. frontal cortex	○	○		✓	✓	

From the left are the age, sex, symptoms, presumed elapsed time since the last onset at the time of the current CT scan, number of lesions for all 23 infarction-positive cases, and the size, location, method of confirmation (DWI/FLAIR) and classification (HAS/EHL/CCL/DWML) of all 77 lesions. As the method of confirmation, a circle (○) denotes that the lesion was confirmed by the image (DWI or FLAIR), a cross (×) denotes that the lesion could not be confirmed on the image, and a negative sign (-) denotes that the image did not exist. Note that patient no. 3 appears twice since two cases were obtained at two different time points from this patient

between with and without TS images were analyzed with the Wilcoxon signed-rank test.

Results

Twenty-nine pairs of brain CT images of 28 patients matched the inclusion criteria by the search through our image database. No pairs matched the exclusion criteria, and six pairs were randomly chosen as training cases. The retrospective review of the remaining 23 pairs by the two radiologists revealed a total of 77 lesions. The 77 lesions comprised 74 brain suspected infarcts in 23 cases and 3 HAS in 3 cases. The 74 infarcts included 5 EHLs, 23 CCLs and 9 DWMLs. The three HAS comprised two hyperdense middle cerebral artery signs and one hyperdense anterior cerebral artery sign. Of the 74 infarcts, 52 (70.3%) infarcts in 22 cases, including 5 EHLs in 5 cases, were confirmed by DWI to be infarcts that developed between the previous and current CTs. Of the remaining 22 infarcts, 13 (17.6%) infarcts in 5 cases were confirmed by FLAIR, 7 (9.5%) infarcts in 1 case were confirmed by future CT, and the remaining 2 (2.7%) infarcts in 2 cases were determined by previous and current CTs only. The mean size of the identified brain infarcts was 15.1 mm ± 18.0, and the number of infarcts per infarction-positive case was 3.2. A detailed list of all positive cases is shown in Table 1, and the statistics of the cases are summarized in Table 2.

The processing time for image registration with LDDMM for each case ranged from 664.2 to 2343 s, while the mean was 1189 s. There were no apparent registration failures.

The FOM, lesion-based sensitivity, case-based sensitivity and specificity, FPC, reading time, and results of the two surveys for the 14 radiologists are shown in Table 3. The mean AFROC plot of all readers is shown in Fig. 2. The FOM improved for all radiologists. The mean FOM significantly improved from 0.528 to 0.737 ($p < 0.0001$). The mean sensitivity on a lesion-based analysis significantly increased from 26.5% (286/1078) to 56.0% (604/1078) ($p < 0.0001$) with the addition of TS images. The mean FPC decreased from 0.243 to 0.153 ($p = 0.239$). The mean sensitivity on a case-based analysis significantly increased from 52.8% (170/322) to 78.0% (251/322) ($p < 0.0001$), and the mean specificity on case-based analysis increased from 83.5% (222/266) to 90.6% (241/266) ($p = 0.346$).

The mean reading time was 173 s without TS and 170 s with TS ($p = 0.925$). The radiologists' confidence in their interpretation (survey 1) improved with TS, but not significantly ($p = 0.733$). The median of the confidence level was 3 for both with and without TS. The median of the usefulness of TS (survey 2) was 4, and the minimum was 3.

The subset, whose positive cases consisted only of infarcts confirmed by DWI, comprised 14 positive cases with 42 infarcts (mean size, 14.1 ± 10.0 mm; number of lesions per infarction-positive case, 3.0) and 19 control cases. The FOM improved for all readers, and its mean significantly improved from 0.521 to 0.750 ($p < 0.0001$). The mean sensitivity on a lesion-based analysis significantly increased from 26.0% (153/588) to 58.5% (344/588) ($p < 0.0001$) with the addition of TS images. The mean FPC decreased from 0.219 to 0.141 ($p = 0.628$). The mean sensitivity on a case-based analysis significantly increased from 50.0% (98/196) to 80.1% (157/196) ($p = 0.047$) (Table 3).

The mean lesion-based sensitivities for HAS ($N = 3$) slightly decreased from 31.0% (13/42) to 28.5% (12/42) ($p = 0.629$), that for EHL ($N = 5$) increased from 34.3% (24/70) to 67.1% (47/70) ($p < 0.001$), that for CCL ($N = 23$) increased from 25.2% (81/322) to 57.1% (184/322) ($p < 0.0001$) and that for DWML ($N = 9$) increased from 19.8% (25/126) to 53.2% (67/126) ($p < 0.001$).

Three representative cases in which the sensitivity improved drastically with the addition of TS CT images are shown in Figs. 3, 4, and 5. The first infarct is a CCL in the right frontal lobe, which was correctly marked by 21% (3/14) of the readers without TS and 100% (14/14) with TS

Table 2 Statistics of all cases used for the observer performance study

	Total				Male				Female						
	Number	Age			Number	Age			Number	Age			Scan interval (days)		
		Mean	SD	Range		Mean	SD	Range		Mean	SD	Range	Mean	SD	Range
All positive patients	23	77.5	16.7	11-92	10	77.0	10.4	60-92	13	77.8	20.7	11-92	300	443	1-1836
DWI-positive only patients	14	74.7	19.6	11-91	7	78.0	8.45	67-91	7	71.4	27.1	11-89	86.3	113	1-302
Negative patients	19	79.3	8.93	49-91	10	79.8	5.07	73-87	9	78.7	12.1	49-91	160	214	3-759

From the left are the number of cases, their age distribution according to their sex, and the scan intervals between the previous and current CT images for each group (all positive, DWI-positive only and control cases). The table includes two positive cases obtained from one female patient. They were treated as independent patients for the calculation of the corresponding values

Table 3 Results of the observer performance study

	All cases (n = 42)															Subset (n = 33)			
	FOM		Sensitivity per lesion		Sensitivity per case		Specificity per case		False positives per case		Reading time (s)		Survey 1		Survey 2	FOM		Sensitivity per lesion	
Reader	Without TS	With TS	Without TS	With TS	Without TS	With TS	Without TS	With TS	Without TS	With TS	Without TS	With TS	Without TS	With TS	With TS	Without TS	With TS	Without TS	With TS
1	0.670	0.869	0.403	0.714	0.652	0.870	0.895	1.000	0.143	0.095	120	150	3	4	4	0.429	0.738	0.241	0.368
2	0.642	0.819	0.364	0.610	0.522	0.696	0.895	0.895	0.071	0.071	179	133	4	4	4	0.310	0.667	0.595	0.747
3	0.617	0.795	0.338	0.688	0.565	0.913	1.000	0.947	0.357	0.214	173	197	2	3	4	0.381	0.738	0.298	0.711
4	0.492	0.721	0.260	0.429	0.609	0.739	0.789	1.000	0.143	0.048	186	109	2.5	5	5	0.262	0.548	0.572	0.626
5	0.576	0.793	0.208	0.610	0.478	0.783	1.000	0.895	0.071	0.095	124	138	3	3	4	0.190	0.571	0.639	0.833
6	0.568	0.646	0.234	0.519	0.522	0.870	0.947	0.789	0.119	0.310	163	126	3	4	4	0.238	0.476	0.333	0.635
7	0.348	0.645	0.195	0.416	0.522	0.739	0.474	1.000	0.762	0.048	301	249	3	3	3	0.167	0.429	0.491	0.786
8	0.290	0.641	0.234	0.649	0.478	0.826	0.263	0.474	1.190	0.738	215	254	3	3	4	0.238	0.762	0.642	0.828
9	0.583	0.862	0.325	0.727	0.609	0.826	0.895	1.000	0.167	0.024	223	221	3	3	3	0.357	0.786	0.635	0.878
10	0.526	0.745	0.182	0.558	0.522	0.783	0.842	0.947	0.071	0.048	132	176	3	3	4	0.214	0.548	0.685	0.893
11	0.623	0.724	0.208	0.468	0.522	0.783	1.000	0.947	0.048	0.119	119	121	3	3	4	0.190	0.500	0.513	0.754
12	0.673	0.812	0.364	0.558	0.565	0.739	1.000	1.000	0.048	0.000	173	177	2	3	4	0.286	0.571	0.584	0.882
13	0.210	0.400	0.117	0.325	0.304	0.522	0.947	0.842	0.024	0.143	138	129	2	2	4	0.167	0.286	0.565	0.784
14	0.544	0.773	0.286	0.571	0.522	0.826	0.737	0.947	0.190	0.190	174	195	3.5	4	4	0.214	0.571	0.496	0.774
Overall	0.526	0.732*	0.265	0.560*	0.528	0.780*	0.835	0.906	0.243	0.153	173	170	3	3	4	0.521	0.750*	0.260	0.585*

From the left are the FOM values, sensitivities per lesion, sensitivities per case, specificities per case, number of false positives per case, reading times and survey results of the 14 readers for all cases (N = 42), and FOM values and sensitivities per lesion for the subset (N = 33). The subset comprises positive cases consisting of DWI-positive infarcts only (N = 14) and control cases (N = 19). All values are mean except for the two surveys, which are medians. An asterisk after the number indicates a significant improvement between without TS and with TS ($P < 0.0001$)

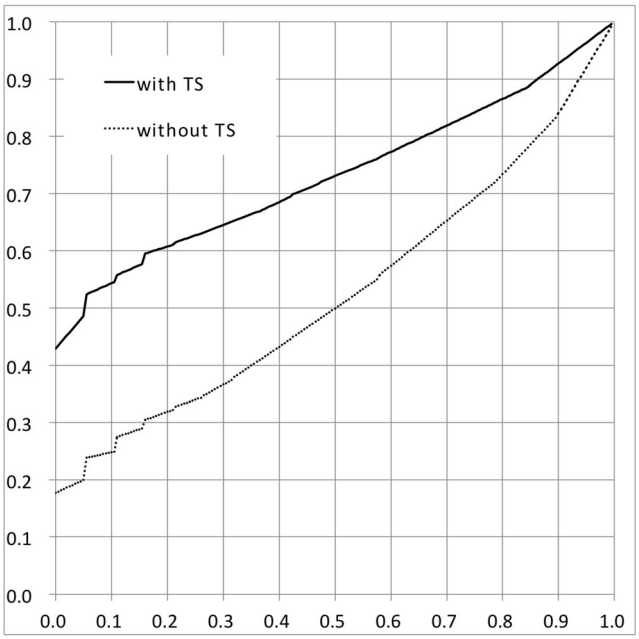

Fig. 2 The mean AFROC plot of all readers. The vertical axis is the lesion localization fraction (equivalent to sensitivity), and the horizontal axis is the false-positive fraction (equivalent to the number of false-positive cases divided by the total number of control cases). The detectability of brain infarctions with TS images is significantly better than that without TS

(Fig. 3). The second infarct is a CCL in the left frontal lobe, which was correctly marked by none of the readers without TS and 93% (13/14) with TS (Fig. 4). The third infarct is an EHL in the left lateral lobe, which was correctly marked by 7.1% (1/14) of the readers without TS and 93% (13/14) with TS (Fig. 5).

On the contrary, three cases demonstrated detrimental effects of TS (i.e., showed a decrease in sensitivity). Two of the cases were an HAS and an EHL in the left cerebral hemisphere. They were both easily noticeable on the current CT, and the decrease in sensitivity was not significant. The other case depicted a fresh infarct in the pons, and 21% (3/14) of the readers were able to mark the lesion correctly without TS but none were able to with TS (Fig. 6).

Discussion

Although the superiority of MRI to CT in the detection of strokes is well established, CT often remains the first choice for suspected stroke patients in clinical practice [8–10]. The main reason for this is probably the advantages of CT such as better accessibility, quicker acquisition time, fewer contraindications and lower cost [10]. Considering the advantages and prevalence of CT scanners, we believe that our result of improved detection of brain infarcts with TS CT images is significant. It is also noteworthy that we recruited as many as 14 readers for the observation performance study, which to our knowledge is unprecedented for this type of study.

The FOM among readers without TS varied from 0.21 to 0.67, and the lesion-based sensitivity varied from 0.12 to 0.40. This large difference probably reflects the fact that the ability to detect infarcts varies greatly among the readers. However, the result that the FOM and sensitivity markedly improved for every reader shows that TS images can enhance this ability regardless of the reader's original detectability of brain infarcts (Table 3).

The mean reading time did not increase with the addition of TS CT images. Along with the improved detectability of brain infarcts and better confidence level and usefulness from the survey, the result suggests that the addition of TS CT images does not pose a burden on the reader as a whole. The question remains as to whether the decrease in time is a result of the readers' reduced viewing time of the current CTs, and, as mentioned earlier, the case with a fresh infarct of the pons, which revealed a detrimental effect of TS, suggests the possibility that this may indeed be true.

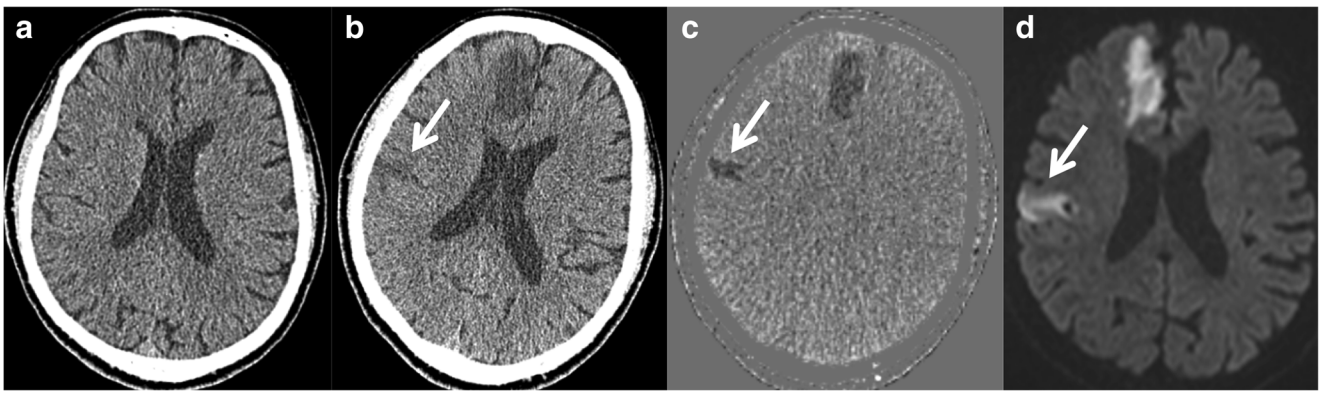

Fig. 3 A case of a 72-year-old male with a fresh infarct in the right frontal lobe (arrow). From the left the (**a**) previous CT, (**b**) current CT, (**c**) TS CT and (**d**) DWI image (B = 1000) are shown. The lesion was correctly marked by 21% (3/14) of the readers without TS and 100% (14/14) with TS. Another fresh infarct is present in the right frontal lobe

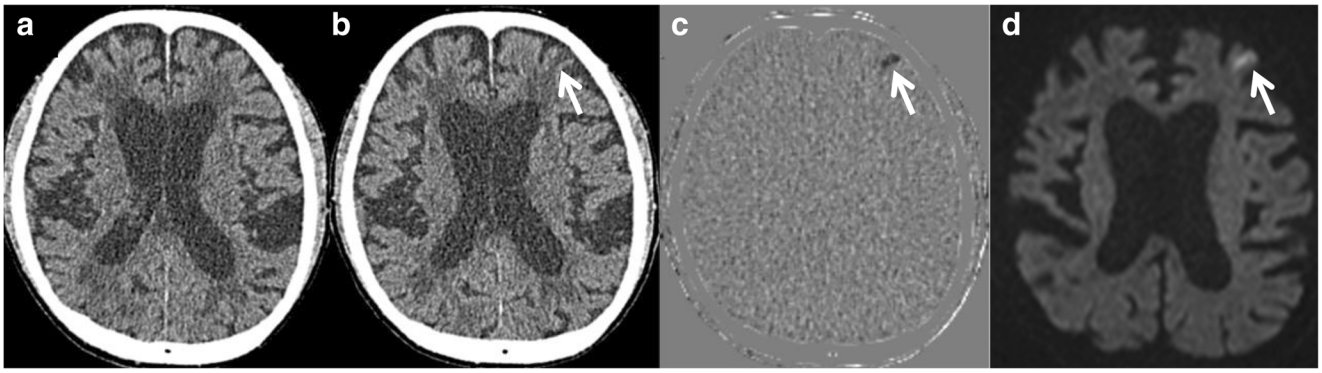

Fig. 4 A case of an 82-year-old male with a fresh infarct in the left frontal lobe (arrow). From the left the (**a**) previous CT, (**b**) current CT, (**c**) TS CT and (**d**) DWI image (B = 1000) are shown. The lesion was correctly marked by none of the readers without TS and 93% (13/14) with TS

The marked improvements in the detectability with TS observed in two CCLs (Figs. 3 and 4) were probably due to the rather peculiar shape and locations of these lesions; they were both elongated and located roughly parallel to the brain sulci, rendering them indistinguishable between infarct and sulci. The TS images were successful in depicting these inconspicuous lesions quite apparently.

As mentioned earlier, CT is prone to beam-hardening artifacts, and they are prominent in the brain stem because of the surrounding skull base [5]. In the case where a detrimental effect was seen in the sensitivity of a fresh pons infarct (Fig. 6), although the lesion was faint, it was detectable on the current CT. However, it was very inconspicuous on the TS image since it had been influenced by the different effects of beam hardening and noise on the current and previous CTs. This is possibly a disadvantage of the current version of the TS technique and needs improvement.

There were several limitations to this study. First, not all infarcts in the image set were confirmed by DWI. We addressed this problem by creating a subset whose positive cases consisted only of infarcts confirmed by DWI. The analysis of this subset revealed significant improvements in the mean FOM, lesion-based and case-based sensitivity and specificity, almost identical to that of the full image set.

Second, although we carefully defined the gold standard, we cannot completely rule out the possibility that the gold standard included other lesions such as demyelinating plaque or encephalitis.

Third, the interpretation session was carried out with thin-slice CT images only. In our interpretation session, the slice thickness of TS CT images was equal to that of the current image (≤ 1 mm), but in a typical clinical setting, brain CT images reconstructed with a thickness of 4 to 5 mm are used as well for interpretation. Although thick-slice CT images (≥ 4 mm) might aid the detection of early CT signs where the contrast between cortex and white matter is vague, it will likely be challenging to detect small infarcts < 5 mm in size. Moreover, a guideline by the American College of Radiology for practice parameters of brain CT states that for brain CT the slice thickness should be no greater than 5 mm and as thin as possible for imaging of the cranial base [19]. A recent study showed that thin-slice (0.625 mm) brain CT yields better detectability of intraluminal thrombus than thick-slice (5 mm) CT [20]. As such, we did not consider this limitation to

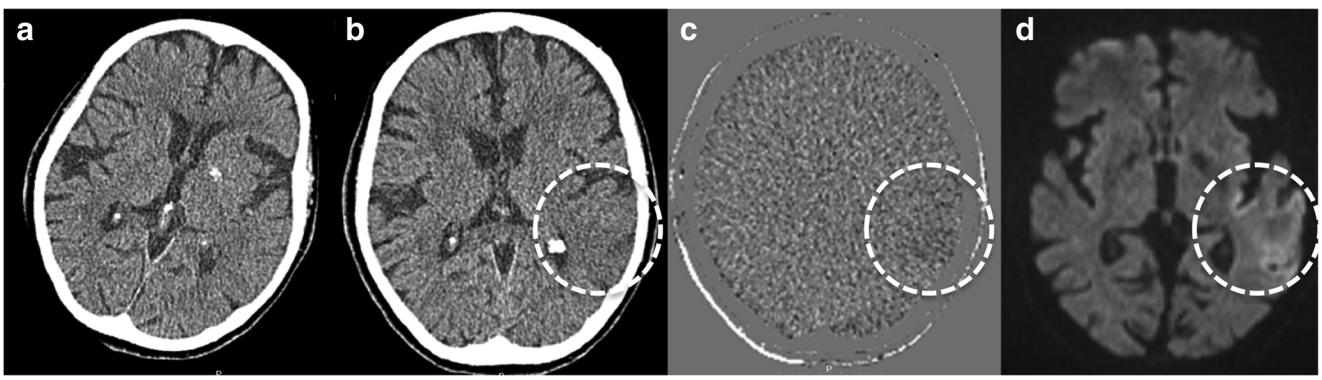

Fig. 5 A case of a 78-year-old female with a fresh infarct in the left lateral lobe (dotted circle). From the left the (**a**) previous CT, (**b**) current CT, (**c**) TS CT and (**d**) DWI image (B = 1000) are shown. The lesion was correctly marked by 7.1% (1/14) of the readers without TS and 93% (13/14) with TS

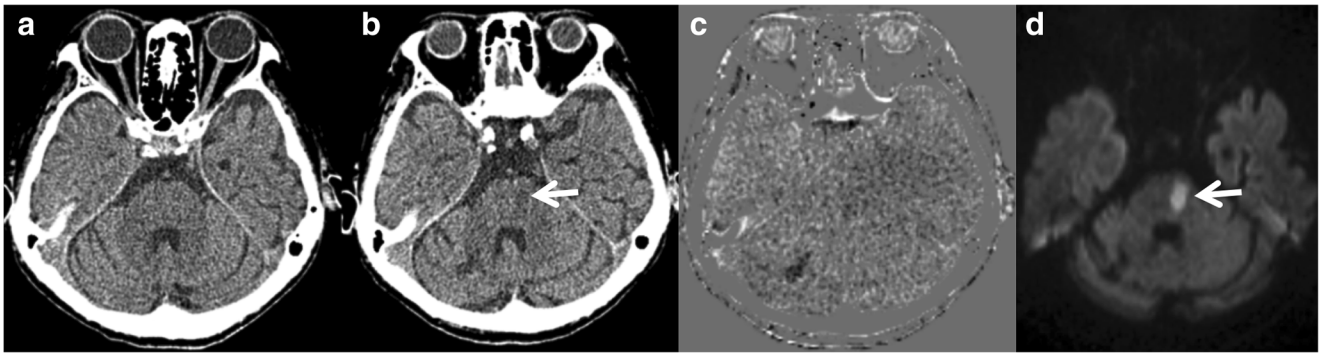

Fig. 6 A case of an 80-year-old female with a fresh infarct in the pons (arrow). From the left the (**a**) previous CT, (**b**) current CT, (**c**) TS CT and (**d**) DWI image (B = 1000) are shown. The lesion was correctly marked by 21% (3/14) of the readers without TS and none with TS. Note how the lesion is inconspicuous on the TS CT, although they are apparent on the current CT and DWI images. An old right cerebellar infarct coexists in the current CT

be critical in our study design. However, it is known that the SNR and CNR increase as the slice thickness of CT images increases [21], so there is a possibility that the detectability of EHLs without TS might have been underestimated. Therefore, it would be premature to conclude that TS CT images significantly improve the detectability of EHLs when thick-slice CT images are used. Future work is necessary to investigate this.

Fourth, to create TS images with our technique, a previous brain CT must be available as thin-slice CT images. Although currently this may not often be the case, we expect that more CT images will be stored as thin-slice CT, and the TS scheme can be more widely applied as the storage cost of images decreases with time and the utility of TS images is recognized.

Lastly, the mean processing time for image registration with LDDMM was approximately 20 min, which is not trivial considering the importance of detecting EHLs in the short time frame allowed. This will hopefully not be a significant problem since the computation time can be expected to decrease drastically when the algorithm is further optimized and the use of GPU is incorporated.

In summary, temporal subtraction CT images significantly improved the detectability of newly developed brain infarcts without compromising interpretation time and showed promise for helping clinicians in their detection.

Funding The author K.T. has received funding from Canon Inc.

Compliance with ethical standards

Guarantor The scientific guarantor of this publication is Kaori Togashi.

Conflict of interest The authors G.A., K.N., Y.I., K.S. and H.Y. declare relationships with the following companies: employees of Canon Inc.

All other authors have no conflicts of interest to disclose.

Statistics and biometry No complex statistical methods were necessary for this paper.

Informed consent Written informed consent was waived by the Institutional Review Board.

Ethical approval Institutional Review Board approval was obtained.

Methodology
- retrospective
- experimental study
- performed at one institution

References

1. Tomura N, Uemura K, Inugami A et al (1988) Early CT finding in cerebral infarction: obscuration of the lentiform nucleus. Radiology 168:463–467. https://doi.org/10.1148/radiology.168.2.3393665
2. Truwit CL, Barkovich AJ, Gean-Marton A et al (1990) Loss of the insular ribbon: another early CT sign of acute middle cerebral artery infarction. Radiology 176:801–806. https://doi.org/10.1148/radiology.176.3.2389039
3. Moulin T, Cattin F, Crépin-Leblond T et al (1996) Early CT signs in acute middle cerebral artery infarction: Predictive value for subsequent infarct locations and outcome. Neurology 47:366–375. https://doi.org/10.1212/WNL.47.2.366
4. Tomsick TA, Brott TG, Chambers AA et al (1990) Hyperdense middle cerebral artery sign on CT: Efficacy in detecting middle cerebral artery thrombosis. AJNR Am J Neuroradiol 11:473–477
5. Barrett JF, Keat N (2004) Artifacts in CT: Recognition and Avoidance. Radiographics 24:1679–1691. https://doi.org/10.1148/rg.246045065
6. Inoue T, Nakaura T, Yoshida M, et al (2017) Diagnosis of small posterior fossa stroke on brain CT: effect of iterative reconstruction designed for brain CT on detection performance. Eur Radiol 27:3710–3715. https://doi.org/10.1007/s00330-017-4773-4
7. Allen LM, Hasso AN, Handwerker J, Farid H (2012) Sequence-specific MR imaging findings that are useful in dating ischemic stroke. Radiographics 32:1285–1297. https://doi.org/10.1148/rg.325115760
8. Chalela JA, Kidwell CS, Nentwich LM et al (2007) Magnetic resonance imaging and computed tomography in emergency assessment of patients with suspected acute stroke: a prospective

comparison. Lancet (London, England) 369:293–298. https://doi.org/10.1016/S0140-6736(07)60151-2
9. Fiebach JB, Schellinger PD, Jansen O et al (2002) CT and diffusion-weighted MR imaging in randomized order: Diffusion-weighted imaging results in higher accuracy and lower interrater variability in the diagnosis of hyperacute ischemic stroke. Stroke 33:2206–2210. https://doi.org/10.1161/01.STR.0000026864.20339.CB
10. Birenbaum D, Bancroft LW, Felsberg GJ (2011) Imaging in acute stroke. West J Emerg Med 12:67–76. https://doi.org/10.1161/STR.0000000000000098
11. Crum WR, Hartkens T, Hill DLG (2004) Non-rigid image registration: theory and practice. Br J Radiol 77:S140–S153. https://doi.org/10.1259/bjr/25329214
12. Aoki T, Oda N, Yamashita Y et al (2011) Usefulness of computerized method for lung nodule detection in digital chest radiographs using temporal subtraction images. Acad Radiol 18:1000–1005. https://doi.org/10.1016/j.acra.2011.04.008
13. Uozumi T, Nakamura K, Watanabe H et al (2001) ROC analysis of detection of metastatic pulmonary nodules on digital chest radiographs with temporal subtraction. Acad Radiol 8:871–878. https://doi.org/10.1016/S1076-6332(03)80766-3
14. Aoki T, Murakami S, Kim H et al (2014) Temporal subtraction method for lung nodule detection on successive thoracic CT softcopy images. Radiology 271:255–261. https://doi.org/10.1148/radiol.13130460
15. Sakamoto R, Yakami M, Fujimoto K et al (2017) Temporal subtraction of serial CT images with large deformation diffeomorphic metric mapping in the identification of bone metastases. Radiology 285:629–639. https://doi.org/10.1148/radiol.2017161942
16. Beg MF, Miller MI, Trouvé A, Younes L (2005) Computing large deformation metric mappings via geodesic flows of diffeomorphisms. Int J Comput Vis 61:139–157. https://doi.org/10.1023/B:VISI.0000043755.93987.aa
17. Swets JA (1979) ROC analysis applied to the evaluation of medical imaging techniques. Invest Radiol 14:109–121. https://doi.org/10.1097/00004424-197903000-00002
18. Chakraborty DP (2013) A brief history of free-response receiver operating characteristic paradigm data analysis. Acad Radiol 20:915–919. https://doi.org/10.1016/j.acra.2013.03.001
19. Jordan JE, Bania MA, Blckham KA, Feiwell RJ, Hetts SW, EGH (2014) Acr – Asnr practice parameter for the performance of computed tomography (CT) of the brain. Am Coll Radiol 1076:1–9
20. Riedel CH, Zoubie J, Ulmer S, et al (2012) Thin-slice reconstructions of nonenhanced CT images allow for detection of thrombus in acute stroke. Stroke 43:2319–2323. https://doi.org/10.1161/STROKEAHA.112.649921
21. Tanaka C, Ueguchi T, Shimosegawa E et al (2006) Effect of CT acquisition parameters in the detection of subtle hypoattenuation in acute cerebral infarction: A phantom study. AJNR Am J Neuroradiol 27:40–45